The gaze stability of 4- to 10-week-old human infants

Eric S. Seemiller
Indiana University School of Optometry, Bloomington, IN, USA

Nicholas L. Port
Indiana University School of Optometry, Bloomington, IN, USA

T. Rowan Candy
Indiana University School of Optometry, Bloomington, IN, USA

The relationship between gaze stability, retinal image quality, and visual perception is complex. Gaze instability related to pathology in adults can cause a reduction in visual acuity (e.g., Chung, LaFrance, & Bedell, 2011). Conversely, poor retinal image quality and spatial vision may be a contributing factor to gaze instability (e.g., Ukwade & Bedell, 1993). Though much is known about the immaturities in spatial vision of human infants, little is currently understood about their gaze stability. To characterize the gaze stability of young infants, adult participants and 4- to 10-week-old infants were shown a dynamic random-noise stimulus for 30-s intervals while their eye positions were recorded binocularly. After removing adultlike saccades, we used 5-s epochs of stable intersaccade gaze to estimate bivariate contour ellipse area and standard deviations of vergence. The geometric means (with standard deviations) for infants' bivariate contour ellipse area were left eye = −0.697 ± 0.534 log($^{\circ 2}$), right eye = −0.471 ± 0.367 log($^{\circ 2}$). For binocular vergence stability, the infant geometric means (with standard deviations) were horizontal = −1.057 ± 0.743 log(°), vertical = −1.257 ± 0.573 log(°). These values were all not significantly different from those of the adult comparison sample, suggesting that gaze instability is not a significant limiting factor in retinal image quality and spatial vision during early postnatal development.

Introduction

Human infants are born with apparent immaturities in spatial vision relative to adults, including reductions in contrast sensitivity and visual acuity (Allen, Tyler, & Norcia, 1996; Atkinson, Braddick, & Moar, 1977; Banks & Salapatek, 1976; Norcia, Tyler, & Hamer, 1990). A number of anatomical and physiological immaturities may contribute to this immature performance. At the first stage of neural processing, for example, immature photoreceptors (decreased foveal cone density and photopigment; Yuodelis & Hendrickson, 1986) are likely to decrease quantum capture and limit spatial resolution (Candy & Banks, 1999). It has been suggested that the infant photoreceptor Nyquist limit is between 4 and 6 times coarser than that of an adult (Banks & Bennett, 1988; Candy, Crowell, & Banks, 1998). Additional immaturities in thalamus and cortex, including immature receptive fields (Zhang et al., 2005), increased neural noise (Brown, 1993; Skoczenski & Norcia, 1998), increased cortical synaptic density (Huttenlocher, 1979, 1999), and decreased myelination (Deoni et al., 2011; Deoni, Dean, O'Muircheartaigh, Dirks, & Jerskey, 2012), may also result in immature response properties, leading to the documented reduction in spatial visual performance.

Given these documented immaturities in sensory processing, one might ask how stably infants can maintain their gaze and, in turn, how any instability might affect the development of visual function. Poor spatial vision, such as found in young infants, may contribute to gaze instability. For example, Ukwade and Bedell (1993) have demonstrated that increased stimulus blur leads to an increase in oculomotor instability in adults. In turn, it has been suggested that gaze instability might also negatively affect spatial vision. For example, Chung, LaFrance, and Bedell (2011) have demonstrated that simulations of infantile nystagmus can affect visual acuity in typical adult observers. Others have demonstrated increased instability of amblyopic eyes relative to fellow eyes in monocular viewing (Gonzalez, Wong, Niechwiej-Szwedo, Tarita-Nistor, & Steinbach, 2012; Subramanian, Jost, & Birch, 2013). The complex interaction between sensory capability and motor control in maintaining fixation and permitting fine spatial reso-

Citation: Seemiller, E. S., Port, N. L., & Candy, T. R. (2018). The gaze stability of 4- to 10-week-old human infants. *Journal of Vision*, *18*(8):15, 1–10, https://doi.org/10.1167/18.8.15.

https://doi.org/10.1167/18.8.15 Received January 11, 2018; published August 28, 2018 ISSN 1534-7362

lution is not fully understood in adults (Collewijn & Kowler, 2008; Rucci & Poletti, 2015).

Fixation stability can be relatively easy to measure in adults. Observers are asked to fixate a small target while variability in their eye position is measured over time (e.g., Krauskopf, Cornsweet, & Riggs, 1960; Stevenson, Sheehy, & Roorda, 2016). Unfortunately, because infants cannot be asked to fixate a target, these measurements become more complex during infancy and early childhood. In the current study, both adult and 4- to 10-week-old infant participants were presented with a dynamic random-noise stimulus updating at 3 Hz. The dynamic random spatial noise patterns were temporally uncorrelated and presented at one viewing distance. Thus, there was no stable feature to drive smooth pursuit or vergence, and so, after the removal of adultlike saccades from the responses, the remaining combination of apparently fixational eye movements could be defined as the gaze stability of the participants. This study represents the first attempt to measure gaze stability during infancy; although our hypothesis was that young infants would have immature stability relative to adults, we found no significant difference between the two groups on the scale at which measurements could be made. Furthermore, there was no significant difference in the stability of horizontal or vertical vergence alignment between the two groups.

Methods

Subjects

Twenty-two typically developing, full-term infants between 4 and 10 weeks postpartum and 13 adults (with no self-reported visual-acuity or binocular-vision abnormalities) were recruited from the local community. Informed consent was obtained from adult participants and the infants' guardians. The study was approved by the Indiana University Institutional Review Board and adhered to the tenets of the Declaration of Helsinki.

Stimulus

Random-noise patterns were presented on a rear-projection screen that preserved circular polarization (Figure 1). These patterns subtended visual angles of 44° vertically and 66° horizontally, from a viewing distance of 65 cm. Because this experiment was performed as part of another project that required dichoptic presentation, the right- and left-eye images were presented using one projector for each eye (Casio XJS 52, Shibuyu, Tokyo), with circular polarizers of opposite direction for the two eyes. The projectors were stacked vertically and their images aligned visually. The red and blue video channels from the stimulus-generation computer were each converted to a signal for the green channel of a projector to generate the binocular green-and-black stimulus. The subjects wore appropriate circular polarizing filters fitted into an age-appropriate spectacle frame. The same stimulus was presented to each eye in this experiment. Through the filters, the luminance of the green pixels was 203 cd/m^2; for black pixels it was 11 cd/m^2. A field of randomly placed green noise elements was drawn on a black background using routines from the Psychophysics Toolbox (Brainard, 1997) and MATLAB (MathWorks, Natick, MA). The noise elements each subtended visual angles of 4° horizontally and 6° vertically. The location of each element was assigned using a uniform random-number generator and could overlap other nearby noise elements. Between 45% and 50% of the screen was green in each frame. The stimulus then refreshed to a new field of static noise elements at 3 Hz.

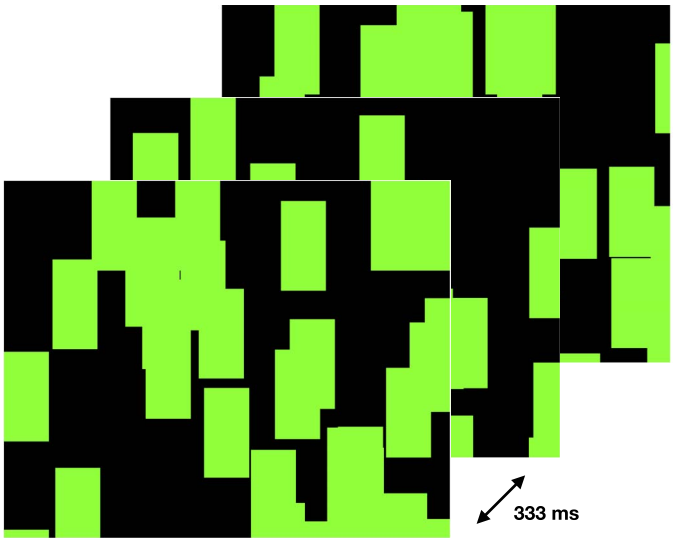

Figure 1. An example of three stimulus frames used in this experiment. The frames updated at 3 Hz for 30 s, so a new frame was presented every 333 ms.

Eye-movement recording

An EyeLink 1000 (SR Research, Ottawa, Canada) Purkinje-image eye tracker was used to record eye position. A longer wavelength light source (940 nm) than is typically provided for this instrument (890 nm) was used to improve data quality for the infant subjects. Though it is unclear why this wavelength improves data quality, it may be due to decreased iris pigment in developing humans (SR Research, personal communication, June 19, 2015). The same wavelength

of light was used for both adult and infant participants. Images of both eyes were captured at 250 Hz using a 16-mm lens (Tamron, Saitama-shi, Saitama, Japan). The sampling rate was reduced from the maximum rate possible (1000 Hz) to 250 Hz to improve the signal-to-noise ratio of each sample. Horizontal and vertical eye positions were calculated using EyeLink software and the EyeLink Toolbox for MATLAB (Cornelissen, Peters, & Palmer, 2002).

The eye tracker was calibrated and validated for each adult observer by having them look at nine fixation targets across the stimulus field, using the EyeLink's dedicated calibration protocol. Because infant fixation could not be guaranteed, no attempt was made to calibrate the instrument for them. Therefore, adult data were calibrated for each subject's own eyes, but the infant data were all calibrated using the same adult (Hirschberg ratio = 20 prism diopters/mm). Infants (1 to 12 months) and adults have been noted to have similar Hirschberg ratios on average (Riddell, Hainline, & Abramov, 1994), and the adult Hirschberg ratio used to calibrate the infant data collection is approximately 91% of the mean adult value. Thus, the mean infant eye movements observed here are likely to be underestimated by an amount on the order of 10%.

Stability analysis

The participants viewed the stimulus for trials lasting 30 s. Adult observers used a chin rest and were asked to look near the center of the screen for the duration of the trial. No instruction could be given to infant observers, but their heads were gently supported in the same position as the adults' relative to the screen.

Data were up-sampled via linear interpolation to 1000 Hz, which is the maximum binocular recording rate of the eye tracker. This permitted smoother implementation of postprocessing algorithms, including removal of blinks and saccades from the data. Blinks were detected and removed using a custom algorithm implemented in MATLAB. After low-pass filtering with a cutoff at 190 Hz, the algorithm detected sequences of abnormally high velocity followed by missing data. The blink removal process then removed an additional 15 ms on either side of the blink.

After filtering out of the blinks, 5-s epochs within the 30-s trials were identified for further analysis. Inclusion criteria for these epochs required that the participant was fixating binocularly within the central 20° of the stimulus, with at most one blink, and that each infant was classified by the experimenters as attentive for the entire interval. The first 5-s epoch that satisfied these constraints was identified for analysis. Saccades were then defined and removed using the properties of an adult saccade (Engbert & Mergenthaler, 2006). Many properties of the developing saccade are largely adultlike from a young age, albeit modulated by attention and amplitude (Hainline, Turkel, Abramov, Lemerise, & Harris, 1984; Salapatek, Aslin, Simonson, & Pulos, 1980), and thus an adult saccade detector is likely to flag a majority of infant saccades. For this experiment, any conjugate binocular eye movement with a velocity greater than 6°/s and a duration greater than 20 ms was flagged. The beginning of the saccade was defined as the sample point immediately before the velocity reached 6°/s, and the end of the saccade was defined as the sample after which the velocity decreased below 6°/s for longer than 100 ms. The intervals between these removed saccades were normalized to the epoch mean and concatenated to form the response vector for further analysis. In order to preserve legitimate gaze variation within the data, epochs with greater than 10 estimated saccades were excluded from further analysis (see Appendix A). This criterion excluded only two infant epochs and no adult epochs. Both infants provided another usable epoch from a different trial.

The stability of gaze position over the 5-s epoch was summarized by calculating the bivariate contour ellipse area (BCEA) for each eye (Timberlake et al., 2005):

$$BCEA = \chi^2 \pi S_H S_V \sqrt{1 - \rho^2}$$

where χ^2 represents the chi-square value corresponding to a probability of 0.95, S_H and S_V are the standard deviations of monocular horizontal and vertical gaze position, and ρ is the Pearson product–moment correlation coefficient between horizontal and vertical gaze position. The BCEA value represents the area of an ellipse drawn around the central 95% of the fitted distribution of eye positions in two dimensions, and thus smaller values mean less variation in eye position (although see Appendix B). Though a number of epochs of stable fixation could occur within an individual's visit, only the epoch with the median BCEA was used for parametric summary analyses.

Horizontal and vertical vergence positions were calculated by subtracting the left eye position from the right eye position at each point in time. Saccades were not removed from each eye's vector because they were defined to be conjugate. Stability of horizontal and vertical vergence was then estimated by calculating the standard deviation of the horizontal and vertical vergence vectors (Stevenson et al., 2016; Van Rijn, Van der Steen, & Collewijn, 1994).

Statistical analyses

Though data were collected over multiple visits, only data from the first visit—or the earliest visit that provided usable data—were included in the hypothesis

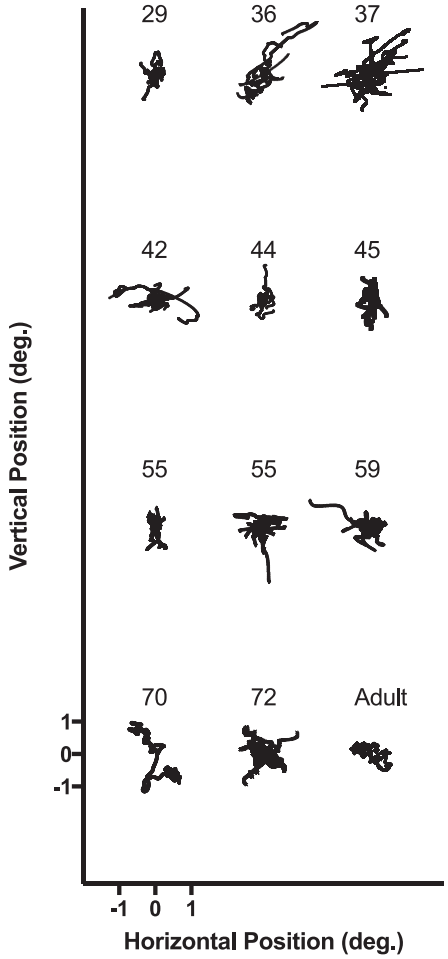

Figure 2. Example gaze-position data from each infant and one adult. If the infant provided multiple usable trials, the median trial is shown. Blinks and saccades were removed. Each trial is offset horizontally and vertically, but the scale in the lower left applies to all trials shown.

testing. The normality of the group data (adults and infants) was confirmed with Shapiro–Wilks tests, using logarithmically transformed data for the BCEA values and vergence standard deviations. Because equal variance could not be assumed, Welch's t test was performed to test the equality of the adult and infant data ($\alpha = 0.05$).

Results

Monocular stability in binocular viewing

Usable data were collected from 11 of 22 infants and 13 of 13 adults. Eleven infant subjects were too restless or sleepy to provide usable data. Figure 2 shows the median BCEA epoch from each infant's youngest visit. Raw horizontal and vertical gaze position from the left eyes of all usable participants are plotted as a function of time (in the event of an even number of trials, the lower BCEA epoch of the two potential median epochs was used for plotting, while the average of the two BCEA values was used for analyses). The median 95% BCEA for each subject is shown in Figure 3. Comparing group means between infants (left: geometric mean ± SD = –0.697 ± 0.534 log($^{\circ 2}$), mean equivalent to 0.470$^{\circ 2}$; right: –0.471 ± 0.367 log($^{\circ 2}$), mean equivalent to 0.475$^{\circ 2}$) and adults (left: –0.450 ± 0.333 log($^{\circ 2}$), mean equivalent to 0.440$^{\circ 2}$; right: –0.522 ± 0.383 log($^{\circ 2}$), mean equivalent to 0.430$^{\circ 2}$) yielded no statistically significant difference for either eye—left: t = 1.328, p = 0.203, 95% confidence interval for the geometric mean difference [–0.146, 0.639]; right: t = 0.331, p = 0.744, 95% confidence interval [–0.051, 0.153]. The group standard deviations were also similar—left: infants = 0.534 log($^{\circ 2}$), adults = 0.333 log($^{\circ 2}$); right: infants = 0.367 log($^{\circ 2}$), adults = 0.383 log($^{\circ 2}$).

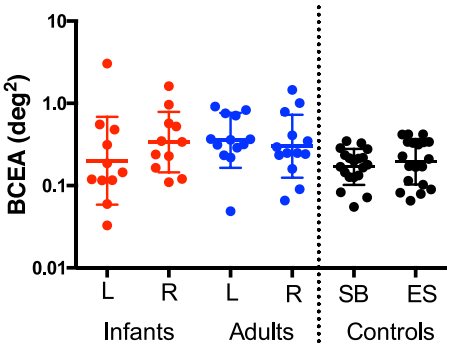

Figure 3. Red and blue values represent the left- and right-eye bivariate contour ellipse area (BCEA) as a function of age group. Each datum is the median 95% BCEA for an infant or adult. Plotted in the far right columns are the results of a control experiment in which two adult subjects were instructed to fixate a small 1° × 1° cross for 20 5-s intervals. The individual BCEA values from the left eyes for all 20 trials are plotted for both of these control subjects. The central horizontal lines represent mean values, with error bars representing 1 standard deviation.

In order to compare these results with a typical fixation stability of adults in a typical study, a control experiment was performed in which two adult subjects (one author and one unaware of the aims of the experiment) were asked to fixate a small fixation cross (1° × by 1°) in the center of the screen in the same conditions as the test condition. Each participant performed this experiment for 20 5-s intervals. The left-eye log BCEAs (geometric mean ± SD) for the two subjects were –0.723 ± 0.08 log($^{\circ 2}$), mean equivalent to 0.189$^{\circ 2}$, and –0.790 ± 0.08 log($^{\circ 2}$), mean equivalent to 0.162$^{\circ 2}$. These mean values are plotted on the right-hand side of Figure 3.

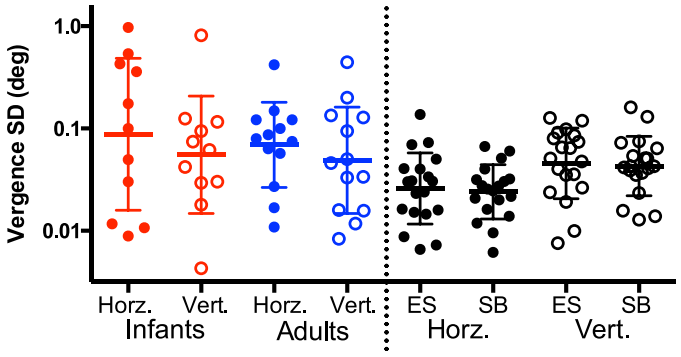

Figure 4. Red and blue data represent the standard deviation of 5 s of horizontal and vertical vergence position as a function of age group. Each datum is the standard deviation of the median trial for individual subjects. Data shown in black represent control trials from two adult subjects fixating on a cross (20 trials per subject). In each case, the left column represents horizontal vergence and the right represents vertical vergence. Error bars are the standard deviation of log-transformed data. There is no statistically significant difference between the age groups.

Binocular stability

On average, neither horizontal nor vertical eye-position measurements were well correlated across the two eyes in either adults or infants, but there was substantial individual variation—horizontal (median correlation coefficients and interquartile ranges): infants = 0.299 (0.092–0.553), adults = 0.374 (−0.190–0.600); vertical: infants = 0.598 (0.275–0.800), adults = 0.620 (0.363–0.857). This is not surprising, as large conjugate eye movements were intentionally removed from the data vectors, leaving some combination of small binocular conjugate, binocular disconjugate, and uncorrelated movements. We defined the disconjugate relationship between the eyes as the vergence stability (though there may be elements of this vector that are not truly vergence). The same eye-position vectors used for monocular analysis were also used for binocular analysis. Horizontal and vertical vergence positions over time were calculated by subtracting one eye's monocular position from the other. Standard deviations of vergence position were calculated for this analysis to estimate vergence stability and were logarithmically transformed for statistical analyses. Figure 4 shows the distribution of standard deviations for horizontal and vertical vergence. The geometric mean of these standard deviations ($\pm SD$) for horizontal vergence for infants was -1.057 ± 0.743 log(°), mean equivalent to 0.087°, and for adults it was -1.156 ± 0.416 log(°), mean equivalent to 0.069°. The corresponding vertical geometric mean ($\pm SD$) for infants was -1.257 ± 0.573 log(°), mean equivalent to 0.055°, and for adults it was -1.311 ± 0.521 log(°), mean equivalent to 0.049°. Neither horizontal ($t = 0.405$, $p = 0.691$) nor vertical ($t = 0.239$, $p = 0.813$) geometric means were significantly different between infants and adults.

Discussion

The results of this study suggest that young infants between 4 and 10 weeks of age as a group are capable of maintaining monocular and binocular gaze in the absence of a consistent fixation target, with median stability at least comparable to that of adults. The infant group-mean log BCEAs and vergence log standard deviations were not significantly different from those of adults and were equivalent to less than a degree squared or a degree in size, respectively. However, there was a greater amount of individual variation in the infant group than in the adult group.

The stimulus format presented here satisfies many of the conditions necessary to compare gaze stability in young infants and adults. Presenting temporally uncorrelated noise patterns to both infants and adults overcame any potential for adults to be more motivated than infants to fixate a small fixation target and removed any stimulus for smooth-pursuit eye movements. Adultlike saccades were removed using a filter. Though the stimuli were presented with the possibility for different images for each eye, they were matched in each frame; therefore, the cues for vertical and horizontal vergence (retinal disparity, proximity, and defocus) were held constant, while the images varied temporally across frames. Despite this complicated and atypical fixation stimulus, the adult BCEA data were comparable to the control fixation condition.

The performance of the young infants with this unnatural stimulus cannot be extrapolated easily to typical viewing. However, given a condition of alert, attentive viewing, tested infants were capable of a period of stable gaze similar to that of the adults reported here and in the adult literature (e.g., Stevenson et al., 2016). This suggests that gaze instability need not be a significant barrier to spatial vision in the developing visual system, provided the infant is in an adequate state of alert attention. The habitual proportion of time that an infant displays this level of performance is unknown, as is the duration of best-quality experience required to drive synaptic tuning and refinement in cortical processes. This experiment is an important first step toward understanding the role of retinal image stability.

One possible explanation for the increased individual variation in the infant data set relates to the inability to calibrate infant eye position individually. As noted in Methods, infants' fixation could not be assumed during

the calibration protocol, and so calibration of an individual adult was used. Though the mean infant Hirschberg ratio is reported to be similar to that of adults, there is greater individual variation in the measured ratio during development (Riddell et al., 1994). Thus the variation in infant BCEA and vergence standard deviations could merely reflect variation in the infant Hirschberg ratio, which may also explain why some infants appear to be more stable than adults in this study. Without an efficient method for performing calibrations for individual infants, it is possible that our calibration procedure under- or overestimated the infant group mean (by using a single adult eye). This adult's Hirschberg ratio was 10% below a typical adult mean value (Riddell et al., 1994), and therefore the infant group mean was most likely to be underestimated. Using a Hirschberg ratio equivalent to 90% of the true value would result in an area being underestimated by approximately 23%. Adding 23% to each infant BCEA value in Figure 3 still does not result in a statistically significant difference between the infant and adult geometric means ($t = 1.27$, $p = 0.216$).

The inability to ask infants to fixate created the need to remove other forms of eye movement from the recording. Removing numerous saccades from the eye-position vector removes one form of variance in eye position. A simulation detailed in Appendix A demonstrated that even after more than 10 saccades of various lengths were removed, estimates of variation in the eye-position vector remained stable and consistent. In the primary analyses, any vector in which more than 10 saccades were flagged was not included.

The saccade-detecting algorithm also looked only for adultlike saccades. Though it has been demonstrated that young infants are capable of making adultlike saccades (Hainline et al., 1984), any immature or slow saccades that were not a part of a stable gaze behavior would not be flagged and would incorrectly be included in our estimation of gaze stability. However, this would only serve to artificially increase apparent instability. Another alternative possibility is that infants' immature fixational microsaccades have similar properties to an adult saccade. If this were true, they would be fixational eye movements that were incorrectly removed from the fixation-stability vector. Furthermore, any epoch containing more than 10 of these saccades would have been removed from the analysis. The characteristics of infant microsaccades remain to be determined.

The control experiment using a simple adult fixation task addressed the relevance of the gaze-stability estimates. The mean values from the two observers were comparable to similar experiments comparing individuals with and without amblyopia using eye trackers. Subramanian et al. (2013) found a larger mean log BCEA of 0.12 log($^{\circ 2}$) when assessing children (5–17 years) over 30-s intervals with a microperimeter. Gonzalez et al. (2012) measured adults for 15-s intervals using an EyeLink 1000 and found log BCEAs of −0.88 log($^{\circ 2}$) for binocular viewing, similar to the numbers found for two adult subjects during our control experiment, in a shorter interval with the same eye tracker: −0.723, −0.790 log($^{\circ 2}$). Additional data from Cherici, Kuang, Poletti, and Rucci (2012) demonstrate that untrained subjects (like those in these experiments) have considerably larger estimates of fixation instability, especially without a defined fixation target, which may also have inflated the adult gaze instabilities measured here.

This study provides insight into the very early development of fixation stability. Though the sensitivity of the current technique suggests that instability of gaze and the resulting retinal image motion may not be a significant immaturity relative to other documented immaturities in spatial vision (e.g., 10-times reduction in visual acuity; Banks & Salapatek, 1976), it is also important to note that a completely stable retinal image impairs the ability to discriminate high spatial frequencies (Boi, Poletti, Victor, & Rucci, 2017; Rucci, Iovin, Poletti, & Santini, 2007; Westheimer & McKee, 1975). Fixational eye movements such as drift have utility in adults' high-acuity vision (Ahissar & Arieli, 2012; Kuang, Poletti, Victor, & Rucci, 2012; Rucci et al., 2007). Though the data collected here are likely to include these eye movements, we are currently unable to determine their role in spatial vision during development.

Keywords: fixation stability, vergence, infants

Acknowledgments

The authors wish to thank Stephanie Biehn for her role in recruiting and working with participants. We must also thank the infants and parents for their patience, time and enthusiasm for this experiment. Funding for this work was provided by NIH R01 EY014660 (TRC) and P30 EY019008 (Indiana University School of Optometry).

Commercial relationships: none.
Corresponding author: Eric S. Seemiller.
Email: eric.seemiller@gmail.com.
Address: Indiana University School of Optometry, Bloomington, IN, USA.

References

Ahissar, E., & Arieli, A. (2012). Seeing via miniature eye movements: A dynamic hypothesis for vision.

Frontiers in Computational Neuroscience, *6*, 89, https://doi.org/10.3389/fncom.2012.00089.

Allen, D., Tyler, C. W., & Norcia, A. M. (1996). Development of grating acuity and contrast sensitivity in the central and peripheral visual field of the human infant. *Vision Research*, *36*(13), 1945–1953.

Atkinson, J., Braddick, O., & Moar, K. (1977). Development of contrast sensitivity over the first 3 months of life in the human infant. *Vision Research*, *17*(9), 1037–1044.

Banks, M. S., & Bennett, P. J. (1988). Optical and photoreceptor immaturities limit the spatial and chromatic vision of human neonates. *Journal of the Optical Society of America A: Optics and Image Science*, *5*(12), 2059–2079.

Banks, M. S., & Salapatek, P. (1976). Contrast sensitivity function of the infant visual system. *Vision Research*, *16*(8), 867–869.

Boi, M., Poletti, M., Victor, J. D., & Rucci, M. (2017). Consequences of the oculomotor cycle for the dynamics of perception. *Current Biology*, *27*(9), 1268–1277, https://doi.org/10.1016/j.cub.2017.03.034.

Brainard, D. H. (1997). The Psychophysics Toolbox. *Spatial Vision*, *10*(4), 433–436.

Brown, A. M. (1993). Intrinsic noise and infant visual performance. In K. Simons (Ed.), *Early visual development, normal and abnormal* (pp. 178–196). New York: Oxford University Press.

Candy, T. R., & Banks, M. S. (1999). Use of an early nonlinearity to measure optical and receptor resolution in the human infant. *Vision Research*, *39*(20), 3386–3398.

Candy, T. R., Crowell, J. A., & Banks, M. S. (1998). Optical, receptoral, and retinal constraints on foveal and peripheral vision in the human neonate. *Vision Research*, *38*(24), 3857–3870.

Cherici, C., Kuang, X., Poletti, M., & Rucci, M. (2012). Precision of sustained fixation in trained and untrained observers. *Journal of Vision*, *12*(6):31, 1–16, https://doi.org/10.1167/12.6.31. [PubMed] [Article]

Chung, S. T. L., LaFrance, M. W., & Bedell, H. E. (2011). Influence of motion smear on visual acuity in simulated infantile nystagmus. *Optometry and Vision Science*, *88*(2), 200–207, https://doi.org/10.1097/OPX.0b013e31820846dd.

Collewijn, H., & Kowler, E. (2008). The significance of microsaccades for vision and oculomotor control. *Journal of Vision*, *8*(14):20, 1–21, https://doi.org/10.1167/8.14.20. [PubMed] [Article]

Cornelissen, F. W., Peters, E. M., & Palmer, J. (2002). The Eyelink Toolbox: Eye tracking with MATLAB and the Psychophysics Toolbox. *Behavior Research Methods, Instruments, & Computers*, *34*(4), 613–617.

Deoni, S. C. L., Dean, D. C., O'Muircheartaigh, J., Dirks, H., & Jerskey, B. A. (2012). Investigating white matter development in infancy and early childhood using myelin water faction and relaxation time mapping. *NeuroImage*, *63*(3), 1038–1053, https://doi.org/10.1016/j.neuroimage.2012.07.037.

Deoni, S. C. L., Mercure, E., Blasi, A., Gasston, D., Thomson, A., Johnson, M., ... Murphy, D. G. M. (2011). Mapping infant brain myelination with magnetic resonance imaging. *The Journal of Neuroscience*, *31*(2), 784–791, https://doi.org/10.1523/Jneurosci.2106-10.2011.

Engbert, R., & Mergenthaler, K. (2006). Microsaccades are triggered by low retinal image slip. *Proceedings of the National Academy of Sciences, USA*, *103*(18), 7192–7197, https://doi.org/10.1073/pnas.0509557103.

Gonzalez, E. G., Wong, A. M., Niechwiej-Szwedo, E., Tarita-Nistor, L., & Steinbach, M. J. (2012). Eye position stability in amblyopia and in normal binocular vision. *Investigative Ophthalmology & Visual Science*, *53*(9), 5386–5394, https://doi.org/10.1167/iovs.12-9941.

Hainline, L., Turkel, J., Abramov, I., Lemerise, E., & Harris, C. M. (1984). Characteristics of saccades in human infants. *Vision Research*, *24*(12), 1771–1780.

Huttenlocher, P. R. (1979). Synaptic density in human frontal cortex: Developmental changes and effects of aging. *Brain Research*, *163*(2), 195–205.

Huttenlocher, P. R. (1999). Dendritic and synaptic development in human cerebral cortex: Time course and critical periods. *Developmental Neuropsychology*, *16*(3), 347–349, https://doi.org/10.1207/S15326942dn1603_12.

Krauskopf, J., Cornsweet, T. N., & Riggs, L. A. (1960). Analysis of eye movements during monocular and binocular fixation. *Journal of the Optical Society of America*, *50*, 572–578.

Kuang, X., Poletti, M., Victor, J. D., & Rucci, M. (2012). Temporal encoding of spatial information during active visual fixation. *Current Biology*, *22*(6), 510–514, https://doi.org/10.1016/j.cub.2012.01.050.

Norcia, A. M., Tyler, C. W., & Hamer, R. D. (1990). Development of contrast sensitivity in the human infant. *Vision Research*, *30*(10), 1475–1486.

Riddell, P. M., Hainline, L., & Abramov, I. (1994). Calibration of the Hirschberg test in human infants. *Investigative Ophthalmology & Visual Science*, *35*(2), 538–543.

Rucci, M., Iovin, R., Poletti, M., & Santini, F. (2007, June 14). Miniature eye movements enhance fine spatial detail. *Nature*, *447*(7146), 851–854, https://doi.org/10.1038/nature05866.

Rucci, M., & Poletti, M. (2015). Control and functions of fixational eye movements. *Annual Review of Vision Science*, *1*, 499–518, https://doi.org/10.1146/annurev-vision-082114-035742.

Salapatek, P., Aslin, R. N., Simonson, J., & Pulos, E. (1980). Infant saccadic eye movements to visible and previously visible targets. *Child Development*, *51*(4), 1090–1094.

Skoczenski, A. M., & Norcia, A. M. (1998, February 12). Neural noise limitations on infant visual sensitivity. *Nature*, *391*(6668), 697–700, https://doi.org/10.1038/35630.

Stevenson, S. B., Sheehy, C. K., & Roorda, A. (2016). Binocular eye tracking with the Tracking Scanning Laser Ophthalmoscope. *Vision Research*, *118*, 98–104, https://doi.org/10.1016/j.visres.2015.01.019.

Subramanian, V., Jost, R. M., & Birch, E. E. (2013). A quantitative study of fixation stability in amblyopia. *Investigative Ophthalmology & Visual Science*, *54*(3), 1998–2003, https://doi.org/10.1167/iovs.12-11054.

Timberlake, G. T., Sharma, M. K., Grose, S. A., Gobert, D. V., Gauch, J. M., & Maino, J. H. (2005). Retinal location of the preferred retinal locus relative to the fovea in scanning laser ophthalmoscope images. *Optometry and Vision Science*, *82*(3), 177–185.

Ukwade, M. T., & Bedell, H. E. (1993). Stability of oculomotor fixation as a function of target contrast and blur. *Optometry and Vision Science*, *70*(2), 123–126.

Van Rijn, L. J., Van der Steen, J., & Collewijn, H. (1994). Instability of ocular torsion during fixation: Cyclovergence is more stable than cycloversion. *Vision Research*, *34*(8), 1077–1087.

Westheimer, G., & McKee, S. P. (1975). Visual acuity in the presence of retinal-image motion. *Journal of the Optical Society of America*, *65*(7), 847–850.

Yuodelis, C., & Hendrickson, A. (1986). A qualitative and quantitative analysis of the human fovea during development. *Vision Research*, *26*(6), 847–855.

Zhang, B., Zheng, J., Watanabe, I., Maruko, I., Bi, H., Smith, E. L., 3rd, & Chino, Y. (2005). Delayed maturation of receptive field center/surround mechanisms in V2. *Proceedings of the National Academy of Sciences, USA*, *102*(16), 5862–5867, https://doi.org/10.1073/pnas.0501815102.

Appendix A

Removing saccades and aligning intersaccade intervals runs the risk of artificially removing legitimate variation in eye position, which is ultimately the measurement of interest in this study. Taken to the extreme, if every other data point were removed and intersaccade intervals were normalized, there would be no variation in the data. The following simulation was performed to determine the point at which removing data would begin to affect estimates of stability.

The average flagged infant saccade in the monocular stability analysis lasted 52 ms ($SD = \pm 18$ ms), and durations were normally distributed. The average adult saccade lasted 46 ms ($SD = \pm 9$ ms). These were not significantly different from one another ($t = 1.60$, $p = 0.113$). The median number of saccades in analyzed epochs was seven for infants (interquartile range = 5–9.5) and one for adults (interquartile range = 0–2.75). To examine the possible effect of saccade number and duration on the results, a 5-s epoch of adult data was identified for which no saccades were flagged. Simulated saccades varying in length between 20 and 100 ms were inserted into this vector at random starting points. If the next starting point was within a simulated saccade, the following new starting point was used. The number of inserted saccades varied between 1 and 50; the length of the entire epoch remained constant at 5 s. The standard deviation of the normalized intersaccade intervals was then computed.

The results of this simulation (Figure A1) demonstrate that estimates of the standard deviation of the processed epoch are consistent and robust to the number and length of saccades until about 10 saccades. Thus, any epoch with more than 10 flagged saccades was not included in the main analysis. It was rare for an individual epoch to have more than 10 saccades: Only two epochs were removed for this reason. Both of these participants provided a usable epoch within the same visit.

Appendix B

If the distribution of eye positions during an epoch is not multivariate normal, bivariate contour ellipse area may not be an appropriate summary of gaze stability. To evaluate this concern, the approach of Cherici, Kuang, Poletti, and Rucci (2012) was also used to summarize the data. Two-dimensional frequency histograms of eye position over an epoch were constructed across a grid of bins ($0.12° \times 0.12°$). Examples are provided in Figure B1.

A cumulative analysis for each individual was then constructed to summarize individual trials. Data were

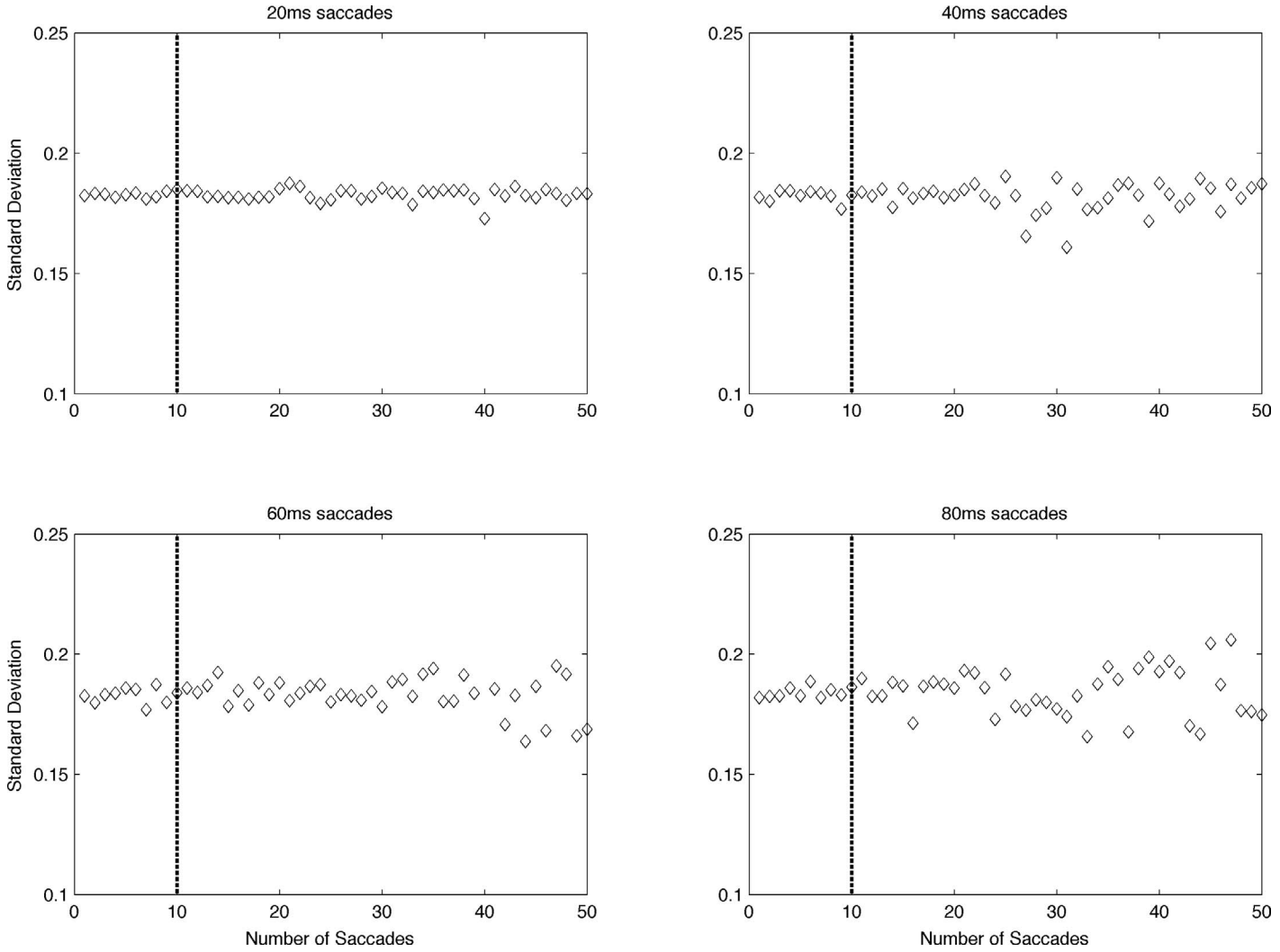

Figure A1. Results of a simulation of the impact of saccade removal and data alignment. Periods of data were removed from a typical adult epoch. Different saccade durations are plotted in each panel, which show the calculated standard deviation in degrees of the remaining aligned data as a function of the number of saccades simulated. Based on this simulation, any epoch containing more than 10 saccades was excluded from the primary analysis.

binned in cells of $0.06° \times 0.06°$, and the frequencies in the cells were rank ordered. These cells were then summed to find the number required to encompass 95% of the position data, the same criterion utilized by Cherici et al. (2012). It should be mentioned that this analysis may not account for positional multimodality in the data; that is, the two most populated bins could be located far apart. Additionally, the temporal information is lost in both forms of stability analysis, as it is not possible to determine whether the eye stayed at one location for a long period of time or returned to that location many times. Examples of these plots are shown in Figure B2.

The area in which 95% of the eye-position distribution fell for each individual was then compared between adults and infants. For adults the mean ($\pm$ *SD*) was $0.181^{\circ 2} \pm 0.064$, and for infants it was $0.248^{\circ 2} \pm 0.107$. These distributions were not statistically significantly different as a function of age ($t = 1.899$, $p = 0.071$). This additional analysis supported the use of the bivariate contour ellipse area for comparison with other studies in the literature and increased our confidence that the normality of the data did not impact the conclusion.

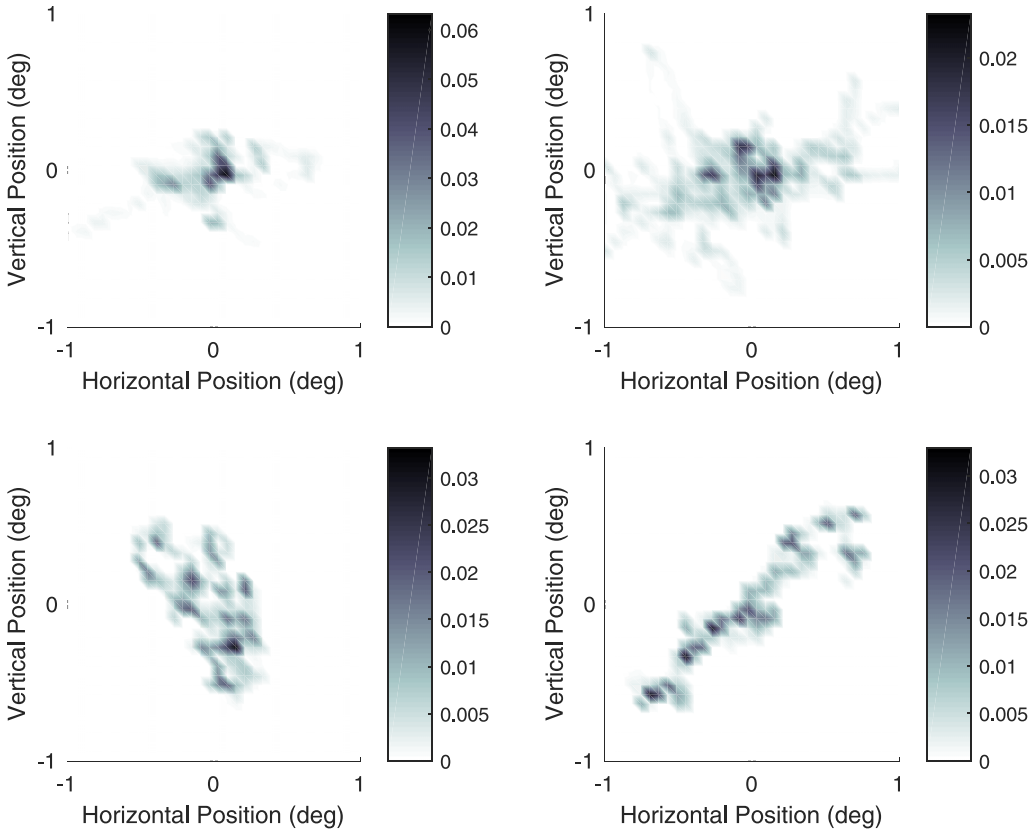

Figure B1. Two-dimensional eye-position distributions for two infants (top) and two adults (bottom). For graphical presentation, bin area is 0.12° × 0.12°. Color bars are normalized to the peak density for each individual plot.

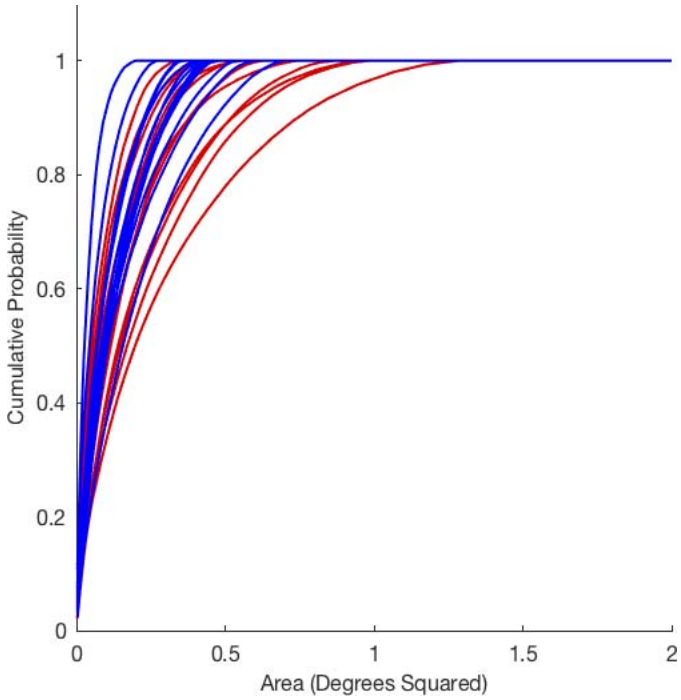

Figure B2. Cumulative probability of eye position as a function of target area for each participant's median trial. Infants are in red and adults are in blue.